Optical Second Harmonic Generation for Size Measurement of Small Spherical Clusters

V. M. Akulin
Moscow Institute of Physics and Technology, Dolgoprudny, Moscow, Russia

E. Borsella * and A. A. Nesterenko†
Comitato Nazionale per la Ricerca e per lo Svillupo dell'Energia Nucleare e delle Energie Alternative, Dipartimento Innovazione, Settore Fisica Applicate, C.R.E. Frascati, P.O. Box 65, 00044 Frascati, Roma, Italy
(Received 26 April 1994)

A new physical effect, the optical second harmonic generation in the combinational process involving a capillary wave excitation, suggests a new diagnostics for the size distribution and temperature of liquid spherical clusters or droplets smaller than the wavelength of light.

PACS numbers: 33.20.Fb, 36.40.+d, 61.46.+w

How does one measure a size distribution of particles smaller than the wavelength of light? This fundamental problem arises in different fields of physics. Presently it becomes important in particular for the remote control of cluster synthesis or for monitoring of cluster vaporization [1], where detailed diagnostics such as electron microscopy or mass spectrometry are inapplicable *in situ* and in real time, whereas the fast and remote optical method [2] of light extinction measures only the mean square cluster radius [3]. In this paper we show that a new physical effect allows us to combine the advantages of optical methods with the high precision of mass spectrometry: One can resolve the size-sensitive capillary oscillation of spherical clusters spectroscopically by means of a multiquantum Raman process.

The weak interaction between mechanical oscillations of a neutral droplet and a light field does not allow one to use the regular Raman process, since in this case one has to detect a weak combinational signal on the top of the wings of the strong line of Rayleigh scattering. The situation becomes completely different when we employ the two-photon Raman process shown in Fig. 1. Indeed, the regular Rayleigh scattering at the pumping frequency ω can be easily separated from the scattered signal near the frequency of 2ω. Moreover, the central symmetry of the droplet does not allow the two-photon Rayleigh process, that is, the scattering at exact double frequency [4]. Only the excitation of the asymmetric oscillation of the droplet shown in Fig. 2 results in a signal at a frequency close to the double frequency of pumping. This oscillation manifests itself in optical spectra via shifts of the frequencies by the analogy to the regular Stokes and anti-Stokes processes.

For droplets of isotropic media the second order nonlinearity $\chi^{(2)}$ comes from the surface [5]. In this paper we therefore concentrate on oscillations of the droplets' surface, that is, capillary waves. We find the eigenfrequencies of the surface modes, perform quantization of this motion, and find the amplitudes of zero vibrations. In the next step we calculate the coupling between the capillary vibrations and the light field and, finally, evaluate the size of the effect.

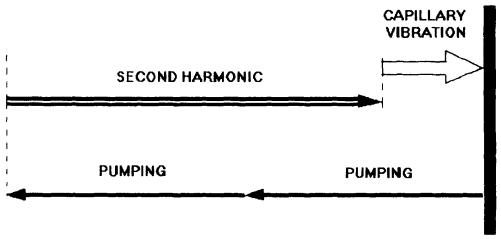

FIG. 1. Parametric excitation of capillary waves in the combinational process of "second harmonic" generation.

We assume that each cluster is a droplet of liquid with density ρ, size R, and surface tension coefficient σ. We describe the hydrodynamics of the droplet by the velocity potential Φ defined as $\vec{v} = \vec{\nabla}\Phi$. The equation of motion

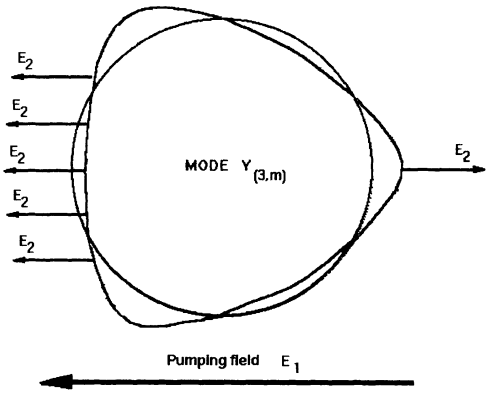

FIG. 2. Generation of the second harmonic at the surface of a droplet. Asymmetric capillary mode $l = 3, m = 0$ is active in the parametric second harmonic generation process. For this mode the total area of the droplet surface normal to the pumping field at the left hand side of the droplet exceeds that from the right hand side. Therefore the overall second harmonic signal generated in phase with the excitation of asymmetric surface oscillation does not vanish.

0031-9007/94/73(9)/1231(4)$06.00

for the potential reads

$$\nabla^2\Phi + \frac{1}{s^2}\ddot{\Phi} = 0, \tag{1}$$

where s is the velocity of sound. We write the solution of this equation in spherical coordinates

$$\Phi = \sum_{n,l,m} c_{n,l,m} r^{-1/2} J_{l+1/2}\left(\frac{\Omega_{n,l}}{s} r\right) \times Y_{l,m}(\theta,\varphi) e^{i\Omega_{n,l}t} \tag{2}$$

in terms of Bessel functions $J_{l+1/2}(x)$ and spherical harmonics $Y_{l,m}(\theta,\varphi)$. Here $c_{n,l,m}$ are the amplitudes of the modes, and the mode frequencies $\Omega_{n,l}$ have to be defined with the help of the boundary conditions

$$\rho\frac{\partial^2\Phi}{\partial t^2}\bigg|_{r=R} = \frac{\sigma}{R^2}\left\{2\frac{\partial\Phi}{\partial r} - \frac{\partial}{\partial r}\left[\frac{1}{\sin\theta}\frac{\partial}{\partial\theta}\left(\sin\theta\frac{\partial\Phi}{\partial\theta}\right) + \frac{1}{\sin^2\theta}\frac{\partial\Phi}{\partial\varphi}\right]\right\}\bigg|_{r=R} \tag{3}$$

discussed in detail in Ref. [6]. Indeed, when we substitute Eq. (2) into Eq. (3) and make use of the relations for Bessel functions $xJ_{\nu-1}(x) + xJ_{\nu+1}(x) = 2\nu J_\nu(x)$ and $J_{\nu-1}(x) - J_{\nu+1}(x) = 2\frac{d}{dx}J_\nu(x)$, we arrive at

$$\frac{\rho\Omega_{n,l}^2 R^2}{\sigma[l(l+1)-2]} = \frac{l+1/2}{R}\frac{J_{l-1/2}(\Omega_{n,l}Rs^{-1}) - J_{l+3/2}(\Omega_{n,l}Rs^{-1})}{J_{l-1/2}(\Omega_{n,l}Rs^{-1}) + J_{l+3/2}(\Omega_{n,l}Rs^{-1})} - \frac{1}{2R}, \tag{4}$$

which implicitly determines the frequencies $\Omega_{n,l}$.

We find the deviation $\zeta(\theta,\varphi)$ of the droplet surface from the equilibrium spherical position via the relation $\dot{\zeta} = v_r|_{r=R} = \frac{\partial}{\partial r}|_{r=R}\Phi$, which yields

$$\zeta = \sum_{n,l,m}\frac{c_{n,l,m}}{\Omega_{n,l}} Y_{l,m}(\theta,\varphi)e^{i\Omega_{n,l}t}\frac{\partial}{\partial r}\bigg|_{r=R}\frac{J_{l+1/2}(\Omega_{n,l}r/s)}{\sqrt{r}}. \tag{5}$$

We can considerably simplify Eqs. (4) and (5) assuming $\Omega_{n,l}Rs^{-1} \ll 1$, which is the case for large clusters. Then only the lowest in n set of frequencies $\Omega_{0,l}$ is important for the capillary waves and hence Eq. (4) reads [6]

$$\Omega_{0,l} \equiv \Omega_l = \sqrt{\frac{\sigma}{\rho R^3}l(l-1)(l+2)}. \tag{6}$$

We find the deviation ζ for this case by replacing Bessel functions $J_{l+1/2}(\Omega_l r s^{-1})$ by $(\Omega_l/2s)^{l+1/2}r^l/\Gamma(l+3/2)$ which yields

$$\zeta = \sum_{l,m} b_{l,m}Y_{l,m}(\theta,\varphi)Re^{i\Omega_l t}, \tag{7}$$

where $b_{l,m} = c_{0,l,m}l(\Omega_l/2s)^{l+1/2}R^{l-2}/\Omega_l\Gamma(l+3/2)$ is the relative amplitude of the mode (l,m).

We now quantize the surface mode. We employ the expression [6]

$$U = \sigma\int\left\{\zeta^2 + \frac{1}{2}\left[\left(\frac{\partial\zeta}{\partial\theta}\right)^2 + \frac{1}{\sin^2\theta}\left(\frac{\partial\zeta}{\partial\varphi}\right)^2\right]\right\} \times \sin\theta\, d\theta\, d\varphi \tag{8}$$

for the potential energy of the surface, substitute here the deviation ζ from Eq. (7), and find the potential energy corresponding to the maximum deviation,

$$U = \frac{\sigma R^2}{2}\sum_{l,m}[2 + l(l+1)]b_{l,m}^2. \tag{9}$$

We now note that the product $\sigma R^2[2 + l(l+1)]$ plays the role of rigidity $\kappa_{l,m}$ for the oscillator of mode l,m and hence via the relation $(b_{l,m})_0 = \sqrt{\hbar\Omega_l/\kappa_{l,m}}$ it yields the relative amplitude

$$(b_{l,m})_0 \equiv \beta_l = \sqrt{\frac{\hbar\Omega_l}{\sigma R^2[2 + l(l+1)]}} \tag{10}$$

of zero vibrations of these modes.

Now we calculate the coupling between the droplet oscillations and the electromagnetic field. We assume that the main contribution to the interaction between the pumping field $\vec{E}_\omega$ and its second harmonic $\vec{E}_{2\omega-\Omega}$ comes from the tensor component of the nonlinear susceptibility $\chi^{(2)}_{n,n,n}$ normal to the droplet surface. Hence the interaction Hamiltonian reads

$$H_{\rm int} = \chi^{(2)}R^2\int(\vec{E}_\omega\vec{n}_\Omega)^2(\vec{E}_{2\omega\pm\Omega}\vec{n}_\Omega)\sin\theta\, d\theta\, d\varphi, \tag{11}$$

where $\vec{n}_\Omega \equiv \vec{n}_\Omega(\theta,\varphi,t)$ is the unit vector normal to the surface oscillating at frequency Ω. For a small perturbation of surface $\zeta \ll R$ we find the components $(n_R, n_\theta, n_\varphi) \cong (1, \frac{\partial\zeta}{\partial\theta}, \frac{1}{\sin\theta}\frac{\partial\zeta}{\partial\varphi})$ of $\vec{n}$ in the spherical coordinates. Substitution of this expression and Eq. (7) into Eq. (11) and integration over the angles φ and θ results in

$$H_{\rm int} = \mathcal{E}_\omega^2\mathcal{E}_{2\omega\pm\Omega}\chi^{(2)}R^2 b_{l,m}f_{l,m}(\alpha), \tag{12}$$

where $\mathcal{E}_\omega$ and $\mathcal{E}_{2\omega\pm\Omega}$ are amplitudes of the field vectors $\vec{E}_\omega$ and $\vec{E}_{2\omega\pm\Omega}$ directed at the angle α with respect to each other, and the function f is given by the expression

$$f_{l,m}(\alpha) = \int\cos\theta\sin\theta\, d\theta\, d\varphi \times\left\{\cos\theta\sin\alpha\cos\varphi\frac{\partial Y_{l,m}}{\partial\varphi} + [\sin\alpha\sin\varphi(\cos^2\theta - 2\sin^2\theta) - 3\cos\theta\sin\theta\cos\alpha]\frac{\partial Y_{l,m}}{\partial\theta}\right\}.$$

Note that the direct product of three vectors $\vec{E}_\omega$, $\vec{E}_\omega$, and $\vec{E}_{2\omega\pm\Omega}$ is a tensor of the third rank. Hence the only nonvanishing contribution to the factor $f(\alpha)$ in the interaction Hamiltonian Eq. (12) comes from the spherical harmonic $Y_{3,m}$, which also represents a spherical tensor of the third rank. We therefore concentrate on the modes with $l = 3$ and find

$$f_{3,0} = \frac{9\pi}{4}\cos\alpha\int_0^\pi \sin^2\theta \times \cos^2\theta(5\sin 3\theta + \sin\theta)d\theta, \quad (13)$$

$$f_{3,1} = f_{3,-1} = -\frac{3\pi}{8}\sin\alpha\int_0^\pi \sin\theta \times [\cos\theta(\cos^2\theta - 2\sin^2\theta) \times (\cos\theta + 15\cos 3\theta) \times \cos\theta(\sin\theta + 5\sin 3\theta)]d\theta,$$

while all other elements vanish.

Now we quantize the interaction Hamiltonian Eq. (12) assuming the pumping field $\mathcal{E}_\omega$ to be classical and take only the terms corresponding to creation of the second harmonic photons. We take into account both positive and negative shifts in frequencies, that is, both Stokes and anti-Stokes processes, and arrive at

$$\hat{H}_{\rm int} = \chi^{(2)}R^2\mathcal{E}_\omega^2\beta_3\sum_m f_{3,m}(\alpha) \times (\mathcal{E}^{(0)}_{2\omega+\Omega}\hat{a}^\dagger_{2\omega+\Omega}\hat{b}_{\Omega,m} + \mathcal{E}^{(0)}_{2\omega-\Omega}\hat{a}^\dagger_{2\omega-\Omega}\hat{b}^\dagger_{\Omega,m}). \quad (14)$$

Here $\hat{b}^\dagger_{\Omega,m}$ and $\hat{b}_{\Omega,m}$ are the creation and the annihilation operators for the capillary mode $l = 3$ of frequency $\Omega = \Omega_3 = \sqrt{30\sigma/\rho R^3}$, and $\mathcal{E}^{(0)}_{2\omega\pm\Omega}$ are the vacuum electric field amplitudes at the frequencies $2\omega \pm \Omega$ corresponding to creation operators $\hat{a}^\dagger_{2\omega\pm\Omega}$ of anti-Stokes and Stokes photons. One can see that the interaction Hamiltonian Eq. (14) has the structure

$$\hat{H}_{\rm int} = \hat{D}_S\mathcal{E}^{(0)}_{2\omega-\Omega}\hat{a}^\dagger_{2\omega-\Omega} + \hat{D}_{aS}\mathcal{E}^{(0)}_{2\omega+\Omega}\hat{a}^\dagger_{2\omega+\Omega}, \quad (15)$$

and hence the operators $\hat{D}_{S,aS}$ play the role of dipole moment operators of clusters. We get the emission rate of Stokes and anti-Stokes photons substituting the moduli squared of these operators averaged over the quantum state of the clusters

$$\langle\hat{D}^\dagger_S\hat{D}_S\rangle = (\chi^{(2)}R^2\mathcal{E}_\omega^2\beta_3)^2\sum_m f_{3,m}(\alpha)^2\langle\hat{b}_{l,m}\hat{b}^\dagger_{l,m}\rangle,$$

$$\langle\hat{D}^\dagger_{aS}\hat{D}_{aS}\rangle = (\chi^{(2)}R^2\mathcal{E}_\omega^2\beta_3)^2\sum_m f_{3,m}(\alpha)^2\langle\hat{b}^\dagger_{l,m}\hat{b}_{l,m}\rangle \quad (16)$$

to the expression $A = 4(2\omega)^3D^2/3\hbar c^3$ for the Einstein coefficient. When we express average products of the surface mode operators $\langle\hat{b}_{l,m}\hat{b}^\dagger_{l,m}\rangle = n_{\rm th} + 1$ and $\langle\hat{b}^\dagger_{l,m}\hat{b}_{l,m}\rangle = n_{\rm th}$ in terms of the thermal number of quanta $n_{\rm th} = (e^{\hbar\Omega/kT} - 1)^{-1}$ we find the probabilities A_S of the Stokes and A_{aS} of the anti-Stokes processes,

$$A_S = \frac{4(2\omega)^3}{3\hbar c^3}(\chi^{(2)}R^2\mathcal{E}_\omega^2\beta_3)^2(n_{\rm th}+1)\sum_m[f_{3,m}(\alpha)]^2,$$

$$A_{aS} = \frac{4(2\omega)^3}{3\hbar c^3}(\chi^{(2)}R^2\mathcal{E}_\omega^2\beta_3)^2 n_{\rm th}\sum_m[f_{3,m}(\alpha)]^2, \quad (17)$$

which are the final results of our analysis.

Let us now evaluate the size of the effect. For a typical metal we estimate $\chi^{(2)} \sim 5\times10^{-15}$ esu, $\rho \sim 5$ g/cm^3, and $\sigma \sim 200$ dyn/cm. Hence for a particle of radius $R = 10^{-6}$ cm we find from Eq. (6) the typical frequency of capillary oscillations $\Omega_3 \sim 4\times10^{10}$ s^{-1}, from Eq. (10) the relative amplitude of zero oscillations $\beta_3 \sim 1.5\times10^{-4}$, and the number of thermal quanta $n_{\rm th} \sim 10^4$. For a pulse Nd-YAG laser of wavelength $\lambda \sim 10^{-4}$ cm with pulse energy $W \sim 20$ mJ and pulse duration $\tau \sim 10^{-8}$ s focused to the area of 0.1 mm^2 we find $\mathcal{E}^2 \sim 8\times10^6$ esu. For the collinear geometry with $\alpha = 0$ the factor $f^2_{3,0}$ is of the order of 50. Substitution of these numbers into Eq. (17) yields $A_SA_{aS} \cong 10^2$ photons/(s cluster). If the concentration of the droplets is such that we have 1 particle per volume of λ^3, the overall emission rate from the focal volume $0.3\times0.3\times1$ mm is about 10^{11} photons/s, that is, 10^3 photons/pulse. This number of photons is sufficient for spectroscopic measurements via photon counting.

We note that since β^2 scales as Ω/R^2 and $n_{\rm th}$ scales as kT/Ω the overall intensity of the second harmonic signal is proportional to R^2T, that is, to the cluster temperature and the area of its surface. We also note that the frequency of the capillary oscillations Ω scales like $R^{-3/2}$, that is, inversely proportional to the square root of the number N of atoms in the cluster. Therefore the spectroscopic method allows us to resolve the individual masses of the clusters if $\delta\Omega/\Omega \sim 1/(2N)$. For the pulse laser $\delta\Omega \sim \tau^{-1}$ and Ω is given by Eq. (6). For the atomic weight of 20 proton masses we substitute the relation $4\pi\rho R^3/3 = 20m_pN$ into Eq. (6) and find the maximum number of atoms in cluster $N_{\rm max} \sim 3\times10^3$ for which the individual N still can be resolved via generation of the second harmonic from the pulsed Nd-YAG laser.

As one of the possible applications of the discussed effect let us consider the diagnostics of size distribution in a CO_2-laser-driven synthesis of Si clusters [7], where the concentration of nanometric liquid clusters is typically of the order of $10^{12} - 10^{13}$ cm^{-3}. The experimental setup sketched in Fig. 3 includes a pulsed dye (or Nd-YAG) laser focused in the reaction zone and a recording scheme for the second harmonic radiation generated there. A gated photon-counting system detects the

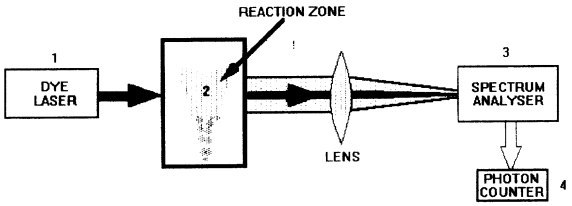

FIG. 3. The experimental setup for diagnostics of the size distribution of clusters in a laser-driven reaction by means of second harmonic generation excitation of capillary oscillations. It includes the following: (1) pulsed dye (or Nd-YAG) laser; (2) reactor; (3) high-resolution spectrum analyzer; (4) gated photon-counting system.

second harmonic signal after it passes through a high-resolution spectrum analyzer. From the spectrum of the second harmonic signal for known values of the density and the surface tension, with the help of the relation $\Omega = \Omega_3 = \sqrt{30\sigma/\rho R^3}$, one gets the size distribution. The estimate done as above for a focused Gaussian pumping beam of wavelength $\lambda \sim 500$ nm, energy $W \sim 7$ mJ, and pulse duration $\tau \sim 10$ ns shows that clusters of radii $R \sim 10^{-6}$ cm emit the net signal of 7×10^3 second harmonic photons per pulse regardless of the diameter of focus. Even by a simple collecting of only 2% of the angulary spreaded second harmonic signal one still gets enough photons for size diagnostics, whereas the situation can be considerably improved via employing the statistical average method.

We conclude by noting that some cluster-chemical reactions such as oxidation or carburization of the surface can also be detected via changing the nonlinear susceptibility $\chi^{(3)}$ associated with the process.

*To whom all correspondence should be addressed.
†Also at General Physics Institute RAS, Moscow, Russia.

[1] Currently clusters are the physical object of great interest; concerning alkali-atom clusters see, for example, D. W. Knight, K. Clemenger, W. A. Heer, W. A. Saunders, M. Y. Chou, and M. L. Cohen, Phys. Rev. Lett. **52**, 2142 (1984); J. Lerme, M. Rollarin, J. L. Vialle, B. Baguenrad, and M. Broyer, Phys. Rev. Lett. **68**, 2818 (1992); V. Näher, H. Göhlich, T. Lange, and T. P. Martin, Phys. Rev. Lett. **68**, 3416 (1992); for nonmetalic clusters see, for example, Y. Suyanna, R. M. Marra, J. S. Haggerty, and H. Hent Bower, Am. Ceram. Soc. Bull. **64** (1984); Y. A. Yang, P. Xia, A. L. Junkin, and L. A. Bloomfield, Phys. Rev. Lett. **66**, 1205 (1991). For the review of modern status of experimental art one can consult *Small Particles and Inorganic Clusters*, edited by C. Chapon, M. F. Gillet, and C. H. Henry (Springer, Berlin, 1989).

[2] Submicron particles, that is, particles comesurated with the wavelength of light can be analyzed with the help of Mie scattering theory. See, for example, A. Ungunt, G. Gerhan, and G. Gouesbet, App. Opt. **20**, 17 (1981). For more details see, for example, M. Kerker, *The Scattering of Light and Other Electromagnetic Radiation* (Academic Press, New York, 1968).

[3] Broad lines of the plasmons do not allow us to use this specific cluster frequency for the size measurement. See, for example, W. T. de Heer, K. Selby, V. Kresin, J. Masu, M. Vollmer, A. Chatelain, and W. D. Knight, Phys. Rev. Lett. **59**, 1805 (1987); W. Hoheisel, K. Jungmann, M. Wollmer, R. Weidenauer, and F. Tager, Phys. Rev. Lett. **60**, 1649 (1988); C. Brechignac, Ph. Cahuzac, N. Kepili, S. Leygnier, and A. Sarfati, Phys. Rev. Lett. **68**, 3916 (1992); **70**, 2036 (1993).

[4] For particles smaller than the wavelength of light the second harmonic generation effect associated with the light propagation is small; see N. Bloembergen, R. K. Chang, S. S. Jha, and C. H. Lee, Phys. Rev. **174**, 813 (1968).

[5] Second harmonic generation is a powerful method for experimental study of surfaces. See, for example, C. D. Chen, A. R. B. de Castro, and Y. R. Shen, Phys. Rev. Lett. **46**, 145 (1981); J. E. Sipe, D. J. Moss, and H. M. van Driel, Phys. Rev. B **35**, 1129 (1987); J. Bloch, G. Lüpke, S. Janz, and H. M. van Driel, Phys. Rev. B **45**, 12011 (1992); X. D. Zhu, Th. Rasing, and Y. R. Shen, Phys. Rev. Lett. **61**, 2883 (1988); T. J. Heinz, C. K. Chen, D. Ricard, and Y. R. Shen, Phys. Rev. Lett. **48**, 478 (1982);C. K. Chen, T. F. Heinz, D. Ricard, and Y. R. Shen, Phys. Rev. Lett. **46**, 1010 (1981);T. F. Heinz, M. M. T. Loy, and W. A. Thompson, Phys. Rev. Lett. **54**, 63 (1985); S. Janz, D. J. Bottomley, and H. M. van Driel, Phys. Rev. Lett. **66**, 1010 (1991). For a more general view, see Y. R. Shen, *The Principles of Nonlinear Optics* (John Wiley, New York, 1984).

[6] L. D. Landau and E. M. Lifshitz, *Fluid Mechanics* (Pergamon Press, Oxford, 1982), p. 239.

[7] For more details of this process see, for example, E. Borsella, S. Botti, E. Giorgi, S. Martelli, S. Turtu, and G. Zeppe, Appl. Phys. Lett. **63**, 1345 (1993), and references therein.

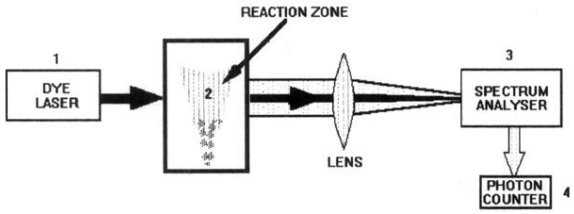

FIG. 3. The experimental setup for diagnostics of the size distribution of clusters in a laser-driven reaction by means of second harmonic generation excitation of capillary oscillations. It includes the following: (1) pulsed dye (or Nd-YAG) laser; (2) reactor; (3) high-resolution spectrum analyzer; (4) gated photon-counting system.